


Article

The *Colletotrichum siamense* Hydrophobin CsHydr1 Interacts with the Lipid Droplet-Coating Protein CsCap20 and Regulates Lipid Metabolism and Virulence

Na Wang [†], Jiyuan Wang [†], Jingwen Lu, Yu Liu, Yitao Xi, Miao Song, Xiaoling Guan, Zhigang Li , Xiao Li, Yu Zhang, Chunhua Lin ^{*} and Weiguo Miao ^{*}

Key Laboratory of Green Prevention and Control of Tropical Plant Diseases and Pests, Ministry of Education, College of Plant Protection, Hainan University, Haikou 570228, China

^{*} Correspondence: lin3286320@hainanu.edu.cn or lin3286320@126.com (C.L.); weiguomiao1105@126.com (W.M.); Tel.: +86-898-66275675 (C.L.)

[†] These authors contributed equally to this work.

Abstract: Previous studies of the lipid droplet-coating protein Cap20 in *Colletotrichum* show that it plays a key role in appressorium development and virulence. In this study, the hydrophobin CsHydr1, which contains a signal peptide of 19 amino acids and a hydrophobic domain (HYDRO), was shown to interact with CsCap20 in *Colletotrichum siamense*. The *CsHydr1* deletion mutant showed slightly enhanced mycelial growth, small conidia, slow spore germination and appressoria formation, cell wall integrity and virulence. Like CsCAP20, CsHydr1 is also localized on the lipid droplet surface of *C. siamense*. However, when CsCap20 was absent, some CsHydr1 was observed in other parts. Quantitative lipid determination showed that the absence of either CsHydr1 or CsCap20 reduced the content of lipids in mycelia and conidia, while the effect of CsCap20 was more obvious; these results suggest that an interaction protein CsHydr1 of CsCap20 is localized on the lipid droplet surface and involved in lipid metabolism, which affects appressorium formation and virulence in *C. siamense*.

Keywords: *Colletotrichum siamense*; hydrophobin CsHydr1; lipid droplet-coating protein CsCap20; appressorial turgor pressure; virulence



Citation: Wang, N.; Wang, J.; Lu, J.; Liu, Y.; Xi, Y.; Song, M.; Guan, X.; Li, Z.; Li, X.; Zhang, Y.; et al. The *Colletotrichum siamense* Hydrophobin CsHydr1 Interacts with the Lipid Droplet-Coating Protein CsCap20 and Regulates Lipid Metabolism and Virulence. *J. Fungi* **2022**, *8*, 977. <https://doi.org/10.3390/jof8090977>

Academic Editor: Laurent Dufossé

Received: 31 July 2022

Accepted: 15 September 2022

Published: 19 September 2022

Publisher's Note: MDPI stays neutral with regard to jurisdictional claims in published maps and institutional affiliations.



Copyright: © 2022 by the authors. Licensee MDPI, Basel, Switzerland. This article is an open access article distributed under the terms and conditions of the Creative Commons Attribution (CC BY) license (<https://creativecommons.org/licenses/by/4.0/>).

1. Introduction

Colletotrichum is a large ascomycete genus that includes numerous important plant pathogenic species and species complexes that infect a wide variety of hosts and cause anthracnose on cereals, legumes, fruit trees, and vegetables [1]. Among them, *C. siamense* was classified into a main phylogenetic clade within the *C. gloeosporioides* species complex and causes anthracnose disease in a wide range of plants. In China, *C. siamense* is reported to be the major pathogenic species of rubber tree *Colletotrichum* leaf disease (CLD) in the field [2–4], which is also the main pathogenic species of anthracnose in many other tropical or subtropical crops, such as *Mangifera indica* [5], *Litchi chinensis* [6], *Camellia chrysantha* [7], *Zizyphus mauritiana* [8], *Alocasia macrorrhiza* [9], *Coffea arabica* [10], and so on. The study of the molecular mechanisms of *C. siamense* pathogenesis may provide a foundation for formulating prevention and control strategies.

In the pathogenic process of many phytopathogenic fungi, including *Colletotrichum* spp., conidia attach to the leaf surface and produce germ tubes, which extend and differentiate into bulbous melanized appressoria [11,12]. Mature appressoria with high turgor pressure are essential to penetrate the leaf surface [13,14]. Lipids are crucial for fungal virulence, from spore germination to the development of mature appressoria. Lipid bodies move into the appressorium during maturation, where they are degraded by triacylglycerol lipase during turgor generation [13,15]. Previous studies have shown that perilipin, a lipid droplet-associated protein, is localized to the lipid droplet surface and is essential to

increase lipid flux into or out of lipid droplets [16]. Perilipin or its homologue is reported to be involved in lipid diseases in mammals and insects. For example, perilipin variants are involved in obesity or leanness in mice, humans, and fruit flies [17–19]. In insect pathogenic fungi, it has also been confirmed that the perilipin homologue MPL1 in *Metarhizium anisopliae* affects lipid metabolism, appressorial turgor pressure and virulence [20]. In a previous study, the *Cap20* gene was cloned and confirmed to be involved in the virulence of *C. gloeosporioides* in avocado and tomato fruits [21]. Moreover, our group has demonstrated that the CsCap20 protein is a perilipin homologue and is involved in the regulation of the number of lipid droplets and appressorium turgor in *C. siamense* from rubber tree [22]. To better understand the regulatory mechanism of CsCap20, interacting proteins, including a hydrophobin, were screened by a yeast two-hybrid system [23].

Hydrophobins (HPs) are small secreted amphiphilic proteins comprising 82–170 amino acids that are only found in filamentous fungi [24–26]; they are hydrophobic and can self-assemble into amphiphilic layers at hydrophilic/hydrophobic or air/water interfaces, allowing fungi to grow into the air from an aqueous environment by reducing the water surface tension [27,28]. Hydrophobins have been proposed to participate in many developmental processes in fungi, including hyphal growth, attachment to hydrophobic surfaces, sporulation, and sexual development [24,29–31]. Some hydrophobins are reported to be involved in fungal virulence, such as MPG1 and MPH1 in *Magnaporthe grisea* [32–35], Hyd1 and Hyd2 in *Beauveria bassiana* [36], and FgHyd2, FgHyd3 and FgHyd4 in *Fusarium graminearum* [31]. Nevertheless, there are no reports on the relationship between hydrophobins and lipid droplet-coating proteins or lipid droplets.

Here, we characterized the function of the hydrophobin CsHydr1, which affects spore germination, appressorium formation and virulence. Additionally, we demonstrated that CsHydr1 interacts with CsCap20, localizes on the lipid droplet surface and influences the lipid content in *C. siamense*; these findings could enrich the understanding of the pathogenic mechanism of hydrophobin in fungi.

2. Materials and Methods

2.1. Fungal Strains and Culture Conditions

The *C. siamense* HN08 strain was used as a wild type (WT) in this study [23,37]. The gene deletion mutant Δ CsCap20 and protein localization strain Cap20-GFP were constructed by our research group previously [22]. The gene deletion mutant Δ CsHydr1, the complementary strain Δ CsHydr1 (*Hydr1*) and the protein subcellular localization strains WT-CsHydr1-*myc* and Δ CsCap20-CsHydr1-*myc* were constructed in this study. For the collection of conidia, hypha was placed and cultured on potato dextrose agar medium (PDA) under continuous fluorescent light for 3–5 days at room temperature. For collection of mycelia, hypha was cultured in liquid complete medium (CM) plates [38].

2.2. CsHydr1 Gene Cloning and Sequence Analysis

The CsCap20 protein of *C. siamense* was used as a bait protein to screen the *C. siamense* yeast cDNA library to obtain partial sequences of CsHydr1 [23]. The CsHydr1 coding regions and upstream and downstream sequences were obtained from the genome database and transcriptome database of HN08 by using a local BLAST search. The primers hydr-F and hydr-R were designed for amplification of the whole coding sequences of CsHydr1 DNA and cDNA. Then cDNA sequence was transformed into an amino acid sequence and analyzed in Modular Architecture Research Tool (SMART, <http://smart.embl-heidelberg.de/>, accessed on 15 May 2022). The phylogenetic tree was constructed by the maximum likelihood method in MEGA6 [39]. The phylogenetic tree was supported with 1000 bootstrap values.

2.3. Protein Secretion Verification of CsHydr1

CsHydr1 (containing full-length cDNA sequences) and CsHydr1^{Δsp} (signal peptide removed, containing only 119 C-terminal amino acid residue sequences) were amplified by Mi-H1-F/Mi-H1-R and Mi-sp-H1-F/Mi-sp-H1-R and ligated to the pSUC2 plasmid

using double digestion (*EcoR* I and *Xho* I) methods, respectively. Primers are presented in Table S1. Then, the recombinant plasmids pSUC2-CsHydr1 and pSUC2-CsHydr1^{Δsp} were transformed into yeast strain YTK12. Thereafter, plate screening and TTC (2,3,5-triphenyl tetrazolium chloride) assays were performed as described by Li et al. [40].

2.4. Targeted Disruption of *CsHydr1* and Complementation

The vector PCX62-S with the sulfonyleurea resistance gene (*ILV1*) was constructed previously in our lab and used as a structure plasmid. The knockout vector PCX62-S-CsHydr1 was constructed by double digestion and homologous recombination methods as described [38]. The schematic diagram is shown in Figure S1a. Approximately 600 bp sequences upstream and downstream of the *CsHydr1* gene were amplified using Hydr-U-F/Hydr-U-R and Hydr-D-F/Hydr-D-R primers, which added the linkers individually (Table S1). Then, the upstream fragment digested by *EcoR* I and *Hind* III were ligated to the N-terminal end of the *ILV1* gene by T₄ ligase to obtain the recombinant plasmid PCX62-S-U. The downstream fragment and the PCX62-S-U vector were digested with *Bam*H I, which were ligated to the C-terminus of *ILV1* using yeast homologous recombination. And the correct vector PCX62-S-CsHydr1 was confirmed by sequencing. Finally, plasmid PCX62-S-CsHydr1 was transformed into protoplasts of HN08 and screened at DCM with 100 μg/mL sulfonyleurea as described previously [22,37,38]. *CsHydr1* deletion mutant was confirmed by PCR with several pairs and Southern blot analysis as shown in Figure S1. Southern hybridization was performed by manual operation of the DIG High Prime DNA Labeling and Detection Starter Kit I (Roche, Basel, Switzerland).

A gene complementation vector was constructed using the PXY203 vector (containing the RP27 promoter and the hygromycin transferase gene *HPH*). The primers PXY203-Hydr1F/R were used to amplify the coding sequence of *CsHydr1* with a homologous linker. Both of PXY203 vector and *CsHydr1* amplified fragment had been digested with *Xho* I and they were co-transferred into yeast XK1-25 for yeast homologous recombination, resulting in PXY203-CsHydr1 plasmid. Then, the plasmid PXY203-CsHydr1 was introduced into the Δ *CsHydr1* mutant protoplasts, and transformants were screened by PDS medium with hygromycin as [38] and verified by PCR, which resulted in complementary strain Δ *CsHydr1* (*Hydr1*). The expression of *CsHydr1* in the Δ *CsHydr1* (*Hydr1*) was followed by the confirmation with RT-PCR using the RT-Hydr1-F/RT-Hydr1-R primer pair. The expression of the *CsHydr1* gene relative to an internal control housekeeping *ACT* gene.

2.5. Validation of Protein Interactions between *CsHydr1* and *CsCap20*

2.5.1. Yeast Two-Hybrid Analysis

The fragment of *CsHydr1*^{Δsp} was cloned into the plasmid pGBKT7, resulting in pGBKT7-CsHydr1^{Δsp}. The whole *CsCap20* fragment was cloned into the plasmid pGADT7, and pGADT7-CsCap20 was constructed (primers are listed in Supplementary Table S1). Then, pGBKT7-CsHydr1^{Δsp} and pGADT7-CsCap20 were co-transformed into yeast Y2H. Next, yeast cells were plated on SD/-Trp-Leu plates and validated by PCR using pGBKT7-F/R and pGADT7-F/R primers. Yeast containing plasmids pGBKT7-CsHydr1^{Δsp} and pGADT7-CsCap20 were dropped on SD/-Trp-Leu and SD/-Trp-Leu-His-Ade plates, pGBKT7-p53+pGADT7-T served as a positive control, and pGBKT7-lam+pGADT7-T was a negative control and then incubated at 30 °C for 3 d to observe yeast growth.

2.5.2. HIS Pull-Down Assay

The recombinant plasmids pGEX-6p-CsHydr1^{Δsp} and pET32a-CsCap20 were constructed by the double digestion method (*Bam*H I and *EcoR* I) (primers are listed in Table S1). His-Cap20 and GST-CsHydr1 fusion proteins were expressed in *E. coli* BL21. Prokaryotic expression, western blot analysis and pull-down assays were performed according to the method described by Wang et al. [23].

2.5.3. Coimmunoprecipitation (Co-IP) Assays

The vector pFL21 and the *CsHydr1* fragment (C-terminus ligated the myc sequence) were digested with *Xho* I and transferred to yeast XK1-25 for yeast homologous recombination. The recombinant plasmid pFL21-*CsHydr1* with *CsHydr1*, myc tag and *hph* (hygromycin resistance gene) was obtained. Plasmid pCB1532-Cap20-GFP was constructed previously [22]. The plasmids pFL21-*CsHydr1* and pCB1532-GFP-Cap20 were co-transformed into HN08, and pFL21-*CsHydr1* was transformed into HN08 as a control. The transformant coexpressing *CsHydr1*-myc and GFP-*CsCAP20* was selected from the wild-type strain on a medium containing both 100 µg/mL sulfonyleurea and 200 µg/mL hygromycin. In addition, the control transformant expressing *CsHydr1*-myc only was obtained from a medium supplemented with 200 µg/mL hygromycin. Finally, the total proteins of these two kinds of transformants were extracted, and the interactions between *CsHydr1*-myc and *CsCap20*-GFP in *C. siamense* were detected by immunoprecipitation and western blotting as described by Wang et al. [23].

2.6. Phenotype Analysis

The spore suspensions of the HN08, $\Delta csHydr1$ and $\Delta csHydr1(Hydr1)$ strains were prepared according to Song et al. [38]. Then, 20 µL spore suspensions (1×10^5 spores/mL) were dropped onto the surface of glass slides, and spores and appressoria were examined under the microscope after incubation at 28 °C according to Song et al. [38]. One hundred spores were counted for each strain. Three independent experiments were performed.

To assay the effects of different stress conditions on tested strains, 10 µL of spore suspension (1×10^5 spores/mL) was inoculated on PDA plates supplemented with sorbitol (1 M), NaCl (1 M), and Congo Red (CR, 100 µg/mL). Colony diameters were measured and photographed after incubation for 5, 7, and 9 days at 28 °C. PDA plates were used as controls. All experiments were carried out in triplicate.

To test the virulence, 20 µL of spore suspensions (1×10^5 spores/mL) of tested strains were dropped on the detached tender leaves with or without wounded as [38] described. Three technical replicated were used for each treatment, and 30 leaves were inoculated for each treatment. The disease lesions were measured and photographed 3 days after inoculation.

2.7. Scanning Electron Microscopy

10 µL of spore suspensions (5×10^5 spores/mL) of the HN08, $\Delta csHydr1$ and $\Delta csHydr1(Hydr1)$ strains were prepared and dropped onto the surface of silicon wafers, respectively. After the droplets were blown dry, the samples were attached to the sample stage with double-sided tape (to avoid contact with the viewing surface of the sample). The Au sputterer was coated to observe the spore surface properties using field emission scanning electron microscopy (Thermo Scientific, Thermo Fisher Scientific, Waltham, MA, USA).

2.8. Immunofluorescence, NR and DiD Staining

The plasmid pFL21-*CsHydr1* was transformed into HN08 and $\Delta csCap20$, and the sub-cellular localization strains WT-*CsHydr1*-myc and $\Delta csCap20$ -*CsHydr1*-myc were obtained. 20 µL of spore suspension (1×10^5 spores/mL) was dropped onto the surface of glass slides, and the localization of *CsHydr1* was observed at different stages.

Immunofluorescence staining: Slides were washed once with $1 \times$ PBS solution, fixed at room temperature for 30 min (4% paraformaldehyde fix solution, Sangon Biotech, Shanghai, China), washed three times with $1 \times$ PBS solution, and subjected to a closed reaction with 1% bovine serum albumin (BSA, Sangon Biotech, Shanghai, China) solution for 1 h at room temperature. The primary antibody reaction with c-Myc (concentration 0.5 µg/mL, Beyotime, Shanghai, China) was performed for 1 h and washed three times with $1 \times$ PBS solution. Then, the fluorescent secondary antibody was immunoprecipitated for 1 h in the

dark and finally washed with $1 \times$ PBS solution three times. The fluorescence channel of GFP was used for observation.

Nil Red staining: After immunofluorescence staining, 100 μ L of Nile Red staining solution (concentration 1 μ g/mL, Solarbio, Beijing, China) was added dropwise to the slide and stained for 6 min at room temperature under dark conditions, followed by three washes with $1 \times$ PBS solution. The fluorescence channel of RFP was used for observation.

DiD staining: After immunofluorescence staining, 100 μ L of DiD staining solution (KeyGen Biotech, Nanjing, China) was added dropwise to the slides and stained for 30 min at 37 °C in the dark, followed by three washes with $1 \times$ PBS solution. The fluorescence of GFP and RFP were observed by using a Nikon confocal microscope (Nikon, Tokyo, Japan).

2.9. Lipid Quantitation

To determine the lipid content, the mycelia of the tested strains were collected from CM for 3 days incubation and conidia were collected from PDA plates for 5 days inoculation by filtration and freeze-dried. 0.5 mL of spore suspension ($1\text{--}1.5 \times 10^8$ spores/mL) and 0.2 g of mycelia of tested strains were prepared and added to separate glass tubes. Quantitative determination of total lipids was assessed by the phosphoric acid-vanillin method according to Wang et al. [20]. A standard curve was generated with triolein (Sangon Biotech, Shanghai, China). Differences in lipid content between treatments were compared using Duncan's analysis of variance (IBM SPSS Statistics 25, Armonk, NY, USA).

3. Results

3.1. The *C. siamense* *CsHydr1* Protein Is a Secreted Protein and Belongs to Class I Hydrophobin

Our previous study showed that hydrophobin (ELA31811.1) is a putative CsCAP20-interacting protein identified by the Y2H system [23]. To confirm their interaction relationship and the biological significance of this hydrophobin, the coding sequence of this hydrophobin was obtained via RT-PCR from the *C. siamense* HN08 strain; this gene putatively encodes a 138-amino-acid protein containing a signal peptide consisting of 19 amino acids at the *N*-terminus and a HYDRO domain at the *C*-terminus of the protein (Figure 1a); its amino acid sequence showed 99% identity to hypothetical hydrophobin of *Colletotrichum* spp. (KAF4805904.1, XP_036491983.1, XP_031884570.1), but low identity with known hydrophobin of other fungi (Figure S2); its cysteine pattern is CN{7}CCN{36}CN{15}C{5}CC{16}C (where N signifies any other amino acid than cysteine). According to Wösten's classification criteria for hydrophobins [41,42], this protein is classified as type I hydrophobin. We named it *CsHydr1* and deposited the sequence in GenBank (Accession No. MN166623).

Since protein *CsHydr1* carries a predicted *N*-terminal signal peptide, we determined its secretory function using the yeast secretion system [43,44]. The full-length (138 amino acids) and *C*-terminal 119 amino acid residue sequences (*CsHydr1* ^{Δ sp}) of the *CsHydr1* gene were fused in vector pSUC2 and then transformed into yeast strain YTK12. The results showed that the full-length sequences of *CsHydr1* and *Avr1b* (positive control) allowed YTK12 to grow on the YPRRA medium (Figure 1b). Meanwhile, the strain transformed with the full-length sequences of *CsHydr1* displayed secreted invertase enzyme activity that catalyzed the reduction of TTC to a red-colored triphenyl formazan (Figure 1b). In contrast, the *CsHydr1* ^{Δ sp} and negative controls (including the untransformed YTK12 strain and YTK12 carrying the pSUC2 vector) did not allow YTK12 strains to grow on YPRRA, and the TTC-treated culture filtrates remained colorless (Figure 1b). Therefore, *CsHydr1* is a secreted protein, and its *N*-terminal signal peptide is required for its secretion.

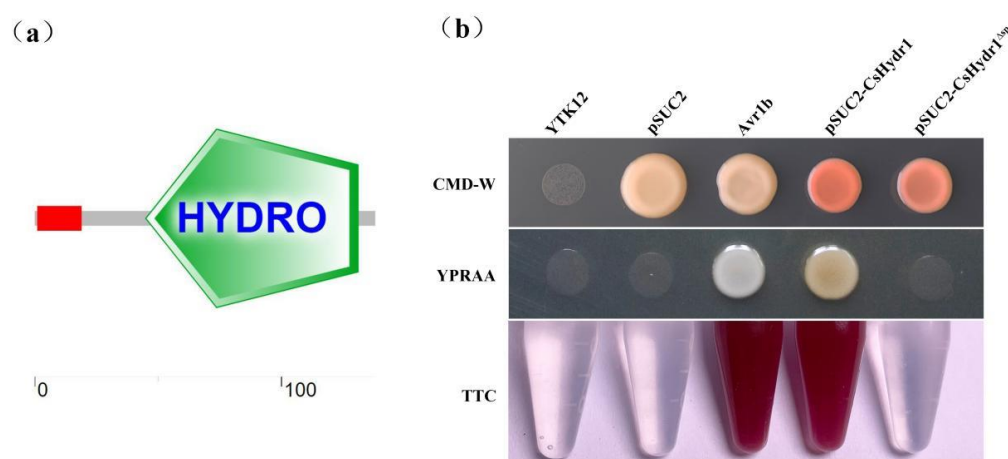


Figure 1. Protein structure and secretion of CsHydr1 in *C. siamense*. (a) SMART analysis of CsHydr1 protein structure. The red region is the signal peptide. The green region is the HYDRO domain; (b) Functional validation of the signal peptide of CsHydr1 using the yeast invertase secretion assay. The full-length and C-terminal amino acid residue sequences without signal peptide (*CsHydr1*^{Δsp}) of the CsHydr1 gene were fused into the pSUC2 vector and transformed into the yeast YTK12 strain. The signal peptide of a known secreted protein Avr1b was used as a positive control. The untransformed YTK12 and YTK12 carrying the pSUC2 vector were used as a negative control. Yeast growth on the CMD-W medium confirmed that the vector had transformed into the yeast cell. The growth in the YPRAA medium and color change of TTC confirmed invertase secretion.

3.2. Targeted Deletion of the *CsHydr1* Gene and Complementation

For gene deletion, 80 transformants were screened by resistance to sulfonylurea in total. Among them, a $\Delta csHydr1$ mutant was confirmed as a *CsHydr1* gene deleted mutant by PCR amplification, sequencing and Southern hybridization analysis (Figure S1). The internal sequence of the *CsHydr1* gene could not be amplified by the primers Hydr-F/Hydr-R, and the products were amplified by the primers Hydr-U-Ou-F/S2R and S1F/Hydr-D-Ou-R in the $\Delta csHydr1$ mutant but not in the wild type, which indicated that *CsHydr1* was replaced by the *ILV1* gene (Figure S1a). In addition, the PCR products from both $\Delta csHydr1$ (4240 bp) and the wild type (1943 bp) using the primers Hydr-U-Ou-F/Hydr-D-Ou-R were confirmed by sequencing (Figure S1a), which showed that the 520-bp open reading frame of the *CsHydr1* gene was replaced by the 2817-bp fragment of the *ILV1* gene, as shown in Figure S1a. The hybridization result showed that only one copy of the *ILV1* gene in the $\Delta csHydr1$ mutant genomic DNA (Figure S1c). Therefore, $\Delta csHydr1$ was indeed a *CsHydr1* null mutant.

Then, the recombination sequence of the open reading frame of the *CsHydr1* gene with the RP27 promoter was reintroduced into the $\Delta csHydr1$ mutant, which resulted in the complementation strain $\Delta csHydr1(Hydr1)$. The $\Delta csHydr1(Hydr1)$ strain was verified by PCR and RT-PCR (Figure S1d,e).

3.3. *CsHydr1* Deletion Mutants Showed Slightly Increased Mycelial Growth, Thin Conidia, Increased Spore Germination Rate and Appressorium Formation Rate

The mycelial growth of the wild-type, $\Delta csHydr1$ mutant, and $\Delta csHydr1(Hydr1)$ was determined under various stress conditions (Figure 2). No significant difference in the morphology of the three colonies was observed. However, the colony diameter was 6.71 ± 0.23 cm after incubation on a PDA medium for 7 days at 28 °C, and those of the wild type and $\Delta csHydr1(Hydr1)$ were 5.96 ± 0.14 cm and 6.03 ± 0.30 cm, respectively. The growth inhibition rate of $\Delta csHydr1$ exposed to 100 $\mu\text{g}/\text{mL}$ Congo Red, 1 M sorbitol and 1 M NaCl was, on average 7.64%, 18.81% and 70.95% higher than that of the wild-type and $\Delta csHydr1(Hydr1)$ strain, respectively. The results indicated that the *CsHydr1* gene affects mycelia growth, cell wall integrity and osmotic sensitivity slightly.

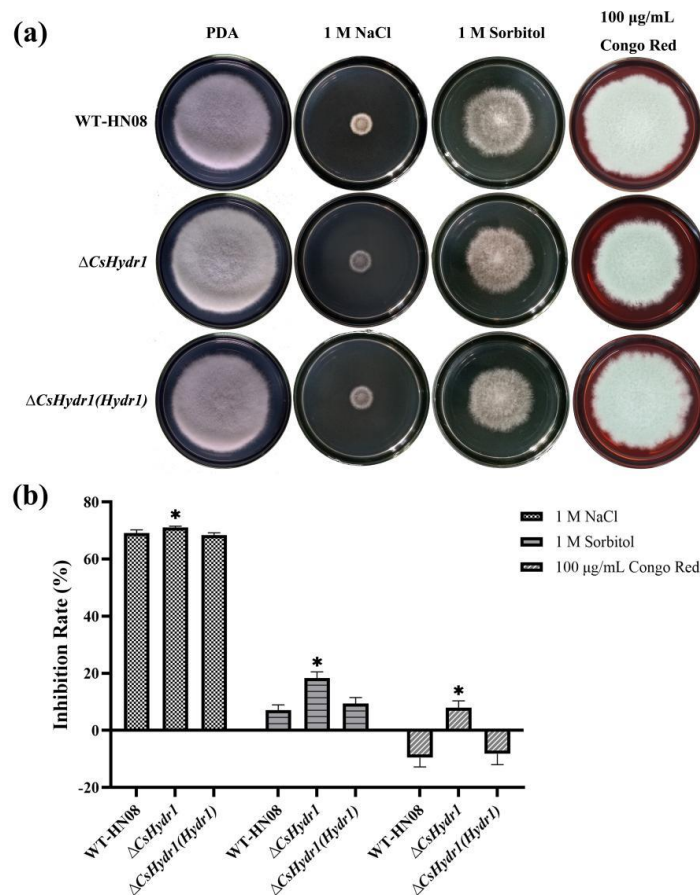


Figure 2. Response of *CsHydr1* mutants to various stress conditions. (a) Growth of the tested strains on PDA plates supplemented with 1 M NaCl, 1 M sorbitol and 100 $\mu\text{g/mL}$ Congo Red for 7 days; (b) Growth inhibition rate of the tested strains under various stresses. The inhibition rate of mycelial growth was calculated using the following formula: Inhibition rate (%) = [(control diameter – treated diameter)/(control diameter \times 100%)]. Each treatment had three replicates. Error bars represent the standard deviations. * indicated significant differences within each measurement group ($p < 0.1$, One-way Anova and Duncan’s test).

The conidia sizes were measured, and the results showed that the sizes of the $\Delta csHydr1$ mutant were $(13.52 \pm 0.32) \times (4.80 \pm 0.13) \mu\text{m}$, and those of the wild-type and $\Delta csHydr1(Hydr1)$ were $(14.07 \pm 0.08) \times (5.41 \pm 0.13) \mu\text{m}$ and $(14.43 \pm 0.25) \times (5.66 \pm 0.07) \mu\text{m}$ (Figure 3a), respectively. The length-width ratio of $\Delta csHydr1$ was slightly larger than that of the other two strains (Figure 3b). The data showed that the $\Delta csHydr1$ mutant had slightly thin conidia.

The rate of spore germination and appressorium formation was tested from 4 h to 12 h after inoculation; it showed that the spore germination rate of $\Delta csHydr1$ was 91% at 6 h, while those of the wild type and $\Delta csHydr1(Hydr1)$ were 64% and 58%, respectively (Figure 3c,d). The appressorium rate of $\Delta csHydr1$ was 57%, while those of the wild type and $\Delta csHydr1(Hydr1)$ were 16% and 17% at 12 h after inoculation, respectively (Figure 3e,f). Which meant the spore germination rate and the appressorium rate of the $\Delta csHydr1$ mutant was higher than those of the wild type and $\Delta csHydr1(Hydr1)$.

Since many hydrophobins are involved in spore superficial rodlet layer formation [25,41,45], we observed the rodlet layer present in the spores of tested strains by scanning electron microscopy. The results showed that the surface of conidia of all three strains was smooth, and no rodlet layers were observed (Figure 4); it was indicated that the function of *CsHydr1* on the formation of rodlets was not obvious. In conclusion, these data indicated that the loss of *CsHydr1* slightly affected the mycelial growth, conidia size, spore germination and appressorium formation rates, but not the rodlet layer of conidia.

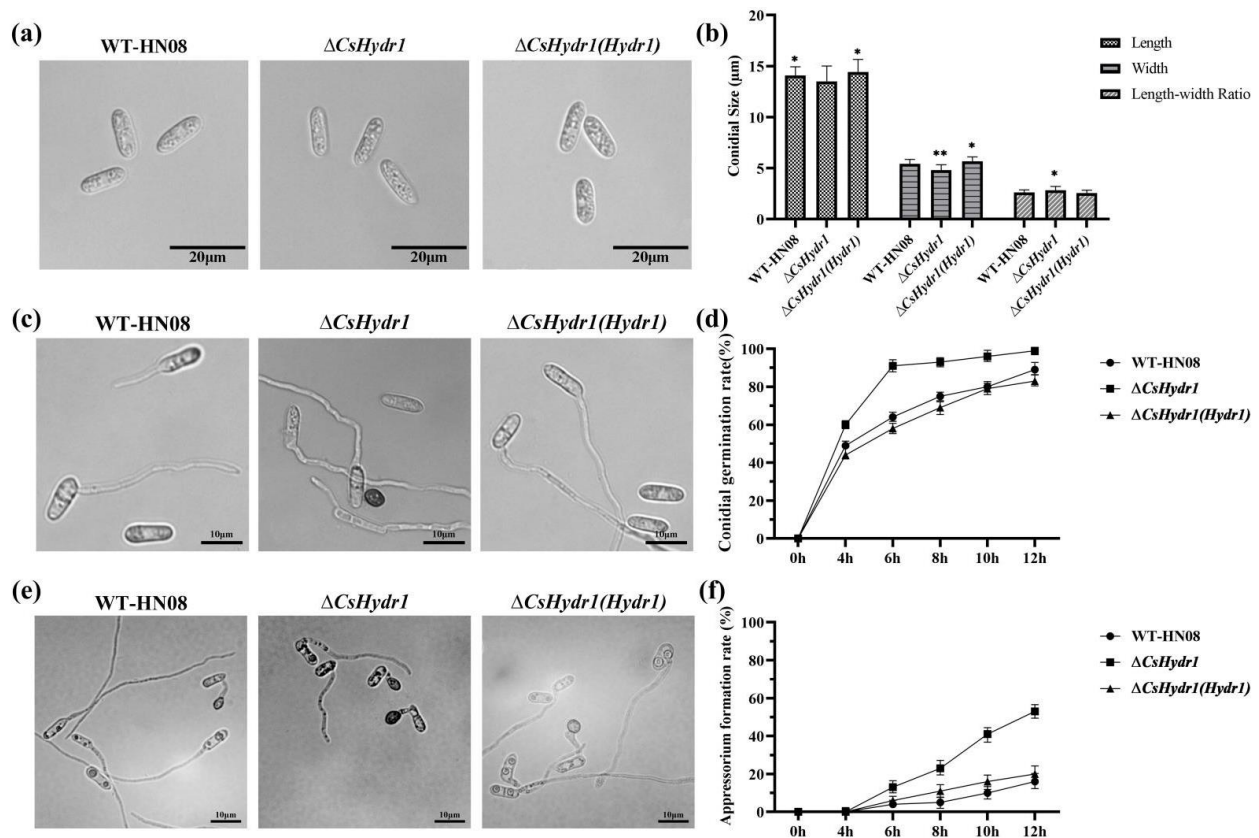


Figure 3. Comparison of conidial size, germination rate and appressorium rate of wild-type HN08, $\Delta csHydr1$ mutant, and $\Delta csHydr1(Hydr1)$ strain. (a,b) are the morphology, and conidial size of the tested strains; (c,d) are morphology and conidial germination rates of the tested strains; (e,f) are morphology and appressorium formation rates of the tested strains. * indicated significant differences within each measurement group (* $p < 0.1$, ** $p < 0.01$, One-way Anova and Duncan's test).

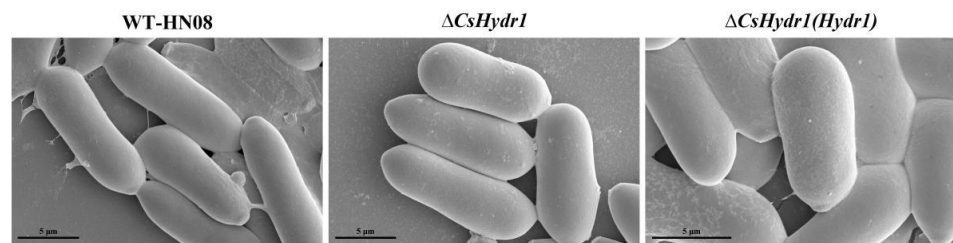


Figure 4. Electron microscopy of spore surfaces of HN08, $\Delta csHydr1$ mutant, and $\Delta csHydr1(Hydr1)$ strain. Bars, 5 μm .

3.4. *CsHydr1* Is Responsible for the Full Virulence of *C. siamense*

The pathogenicity of the wild-type HN08 strain, $\Delta csHydr1$ mutant, and strain $\Delta csHydr1(Hydr1)$ were comparable on healthy light green rubber tree leaves that were wounded or nonwounded. The lesion area and infection rate were measured after 5 days of inoculation (Figure 5). On the wounded leaves, all three strains caused symptoms, and the diseased area caused by $\Delta csHydr1$ (mean $0.71 \pm 0.37 \text{ cm}^2$) was slightly smaller than those caused by the HN08 strain (mean $0.95 \pm 0.36 \text{ cm}^2$) and $\Delta csHydr1(Hydr1)$ strain (mean $0.89 \pm 0.38 \text{ cm}^2$). On the nonwounded leaves, the infection rate of $\Delta csHydr1$ (65.63%) was significantly lower than those of the HN08 strain (93.75%) and $\Delta csHydr1(Hydr1)$ strain (93.75%), and the diseased area caused by $\Delta csHydr1$ (mean $0.46 \pm 0.38 \text{ cm}^2$) was also slightly smaller than those of HN08 strain (mean $0.77 \pm 0.43 \text{ cm}^2$) and $\Delta csHydr1(Hydr1)$ strain (mean $0.75 \pm 0.42 \text{ cm}^2$). The results illustrated that the lack of *CsHydr1* affects fungal virulence to some extent.

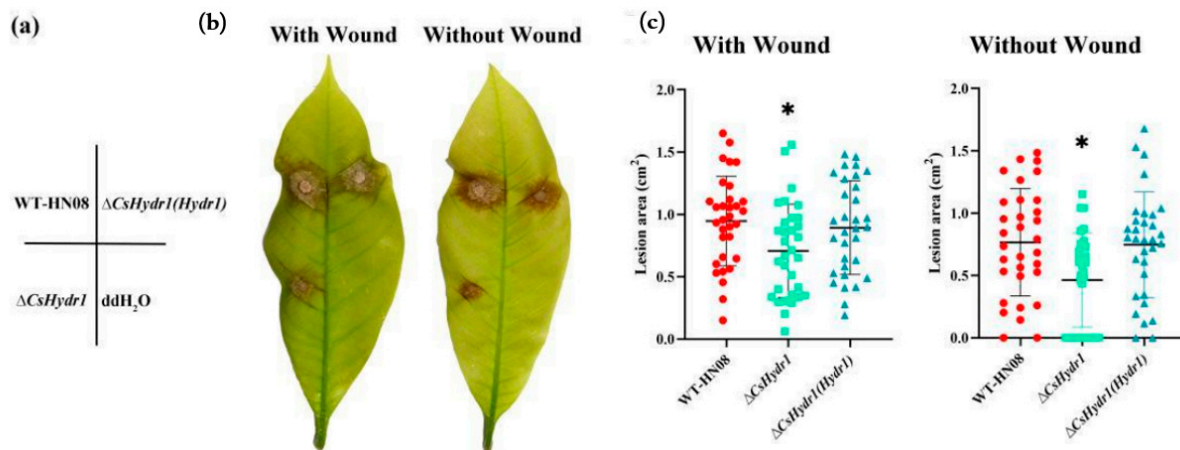


Figure 5. Virulence assays on rubber tree leaves. (a) Schematic diagram of the virulence assays of the tested strains. The rubber tree leaves were inoculated with 20 μ L of conidial suspension (1×10^5 spores/mL) of tested strains through unwounded and wounded ways; The symptoms (b) and dot plot analysis of the lesion areas (c) were shown at 5 days after inoculation. Thirty leaves were inoculated per treatment (* $p < 0.1$, according to one-way ANOVA and Duncan's test; the error bar shows the standard deviation value).

3.5. The Protein CsHydr1 Interacts with CsCap20

To confirm the interaction relationship between CsHydr1 and CsCap20, a yeast two-hybrid system assay was conducted firstly. The results are shown in Figure 6a. All yeast colonies cotransformed with pGBKT7-CsHydr1 ^{Δ SP} and pGADT7-CsCap20, negative control pGBKT7-Lam and pGADT7-T, or positive control pGBKT7-p53 and pGADT7-T grew on SD/-Trp/-Leu. Only yeast colonies co-transformed with pGBKT7-CsHydr1 ^{Δ SP} and pGADT7-CsCap20, and the positive controls pGBKT7-p53 and pGADT7-T could grow on SD/-Trp/-Leu/-His/-Ade (Figure 6a); this result preliminarily verified the interaction between CsHydr1 ^{Δ SP} and CsCap20.

Secondly, recombinant His-CsCap20 protein and GST-CsHydr1 protein were purified and subjected to a His pull-down experiment. The experimental group comprised His-CsCap20 protein and GST-CsHydr1 protein. The positive control group comprised GST-CsHydr1, and the negative control group comprised HIS protein and GST-CsHydr1. The results confirmed that the CsHydr1 protein interacts with CsCap20 (Figure 6b).

Finally, the interaction between CsHydr1 and CsCap20 in vivo was further verified by the Co-IP method. The transformant coexpressing CsHydr1-myc and GFP-CsCap20, and the control transformant expressing CsHydr1-Myc only were obtained. The total proteins of these transformants were extracted and detected by immunoprecipitation and western blot. The results showed that the experimental group CsHydr1-Myc successfully pulled down GFP-CsCap20 from total protein, whereas no interaction with GFP-CsCap20 in the control was observed (Figure 6c). Thus, the interaction of CsHydr1 with CsCap20 was verified in vitro and in vivo.

3.6. Protein CsHydr1 and CsCap20 Both Localize on Lipid Droplet Surface

Immunofluorescence (IF) staining was performed to measure the subcellular localization of the CsHydr1 protein. The recombination plasmid pFL21-CsHydr1 containing a myc tag was constructed. Then, it was introduced into wild-type HN08 and produced the transformant WT-CsHydr1-myc. The transformant WT-CsHydr1-myc underwent immunofluorescence staining using antibodies against c-Myc and analyzed for Myc, NR and DiD signals using epifluorescence microscopy. The results showed that CsHydr1 localized on the lipid droplets in conidia, germ tubes and appressoria (Figure 7a); this subcellular localization of CsHydr1 was consistent with a previous report of CsCap20 (Figure 7b) [22].

CsHydr1 interacted with CsCap20, and both the two proteins localized on the lipid droplets. We wanted to determine whether CsCap20 influenced the subcellular localization of CsHydr1. We introduced the plasmid pFL21-CsHydr1 into $\Delta csCap20$ and resulted in the transformant $\Delta csCap20$ -CsHydr1-myc. Similar to WT-CsHydr1-myc, the CsHydr1 protein is mainly localized on lipid droplets. However, we could clearly observe that some CsHydr1 localized on other parts in addition to lipid droplets when CsCap20 was absent (Figure 7c); these data suggested that CsHydr1 mainly localized to intracellular lipid droplets, and protein CsCap20 was helpful for the localization of CsHydr1 on lipid droplets in *C. siamense*.

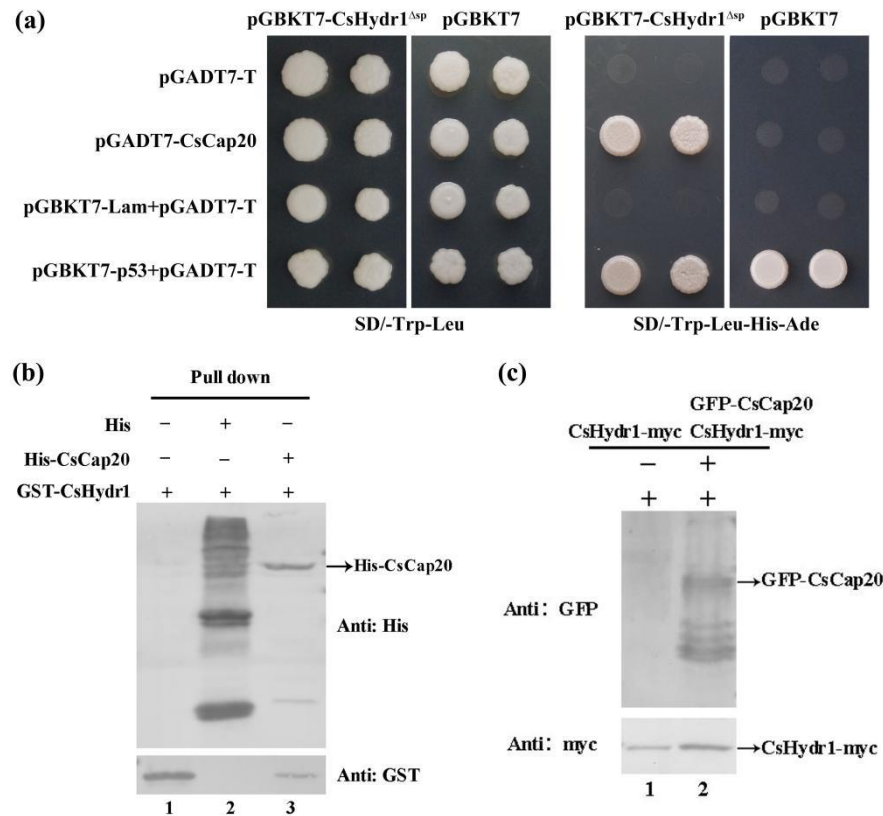


Figure 6. Identification of the interaction between CsHydr1 and CsCap20. (a) Confirmation of the interaction between pGADT7-CsCap20 and pGBKT7-CsHydr1^{Δsp} by yeast two-hybrid assay. pGBKT7-p53+pGADT7-T is the positive control; pGBKT7-Lam+pGADT7-T is the negative control; (b) HIS pull-down results between His-CsCap20 and GST-CsHydr1. Lane 1 is positive control of GST-CsHydr1; Lane 2 is negative control 6 × His null protein and GST-CsHydr1 protein; Lane 3 is His-CsCap20 protein and GST-CsHydr1 protein; (c) Co-IP results between GFP-CsCap20 and CsHydr1-myc. Lane 1 is the control protein from the transformant expressing CsHydr1-myc only; Lane 2 is the protein from the transformant expressing both GFP-CsCap20 and CsHydr1-myc. +, protein added, −, protein not added.

3.7. Deletion of the CsHydr1 or CsCap20 Genes Decreased the Lipid Content in *C. siamense*

A previous study showed that Cap20 of *C. gloeosporioides* and the homologous protein MPL1 of *M. anisopliae* regulated lipid metabolism and decreased the total lipids in a gene deletion mutant [20,22]. Based on both CsHydr1 and CsCap20 being localized to lipid droplets, we also quantitatively determined the lipid content on conidia and mycelia of all of the wild types, $\Delta csHydr1$ and $\Delta csCap20$ (Figure 8). The results showed that the lipids on the conidia and mycelia of HN08 were 572.92 ± 3.36 mg/dL. OD and 698.24 ± 3.95 mg/dL, respectively. Compared with HN08, the lipid content was significantly decreased in both $\Delta csHydr1$ (475.87 ± 18.17 mg/dL. OD in conidia, 605.96 ± 3.45 mg/dL in mycelium) and $\Delta csCap20$ (299.71 ± 1.70 mg/dL. OD in conidia, 381.58 ± 2.17 mg/dL in mycelium); these

data indicated that the absence of *CsHydr1* or *CsCap20* both reduced the content of lipids in mycelia and conidia, while the effect of *CsCap20* was more obvious.

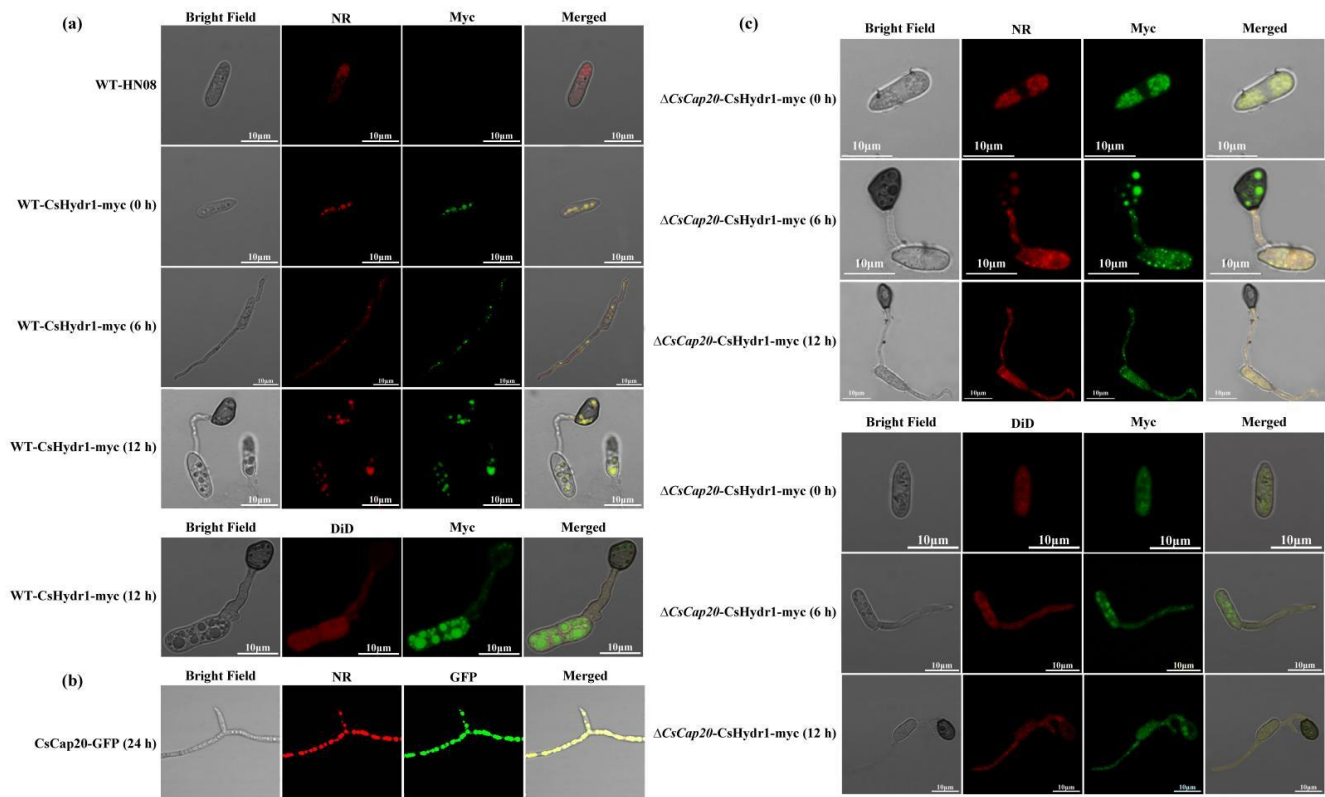


Figure 7. Subcellular localization of the *CsHydr1* protein in WT and $\Delta csCap20$. (a) Protein *CsHydr1* localization in WT. (b) Protein *CsCap20* localization in WT HN08. (c) Protein *CsHydr1* localization in $\Delta csCap20$. WT-*CsHydr1*-myc, the fusion protein *CsHydr1*-myc expressing in wild-type HN08; *CsCap20*-GFP, the fusion protein expressing in wild-type HN08; $\Delta csCap20$ -*CsHydr1*-myc, the fusion protein *CsHydr1*-myc expressing in the $\Delta csCap20$ mutant; Myc, immunofluorescence staining using antibodies against c-Myc; NR, Nile red staining; DiD, DiD staining.

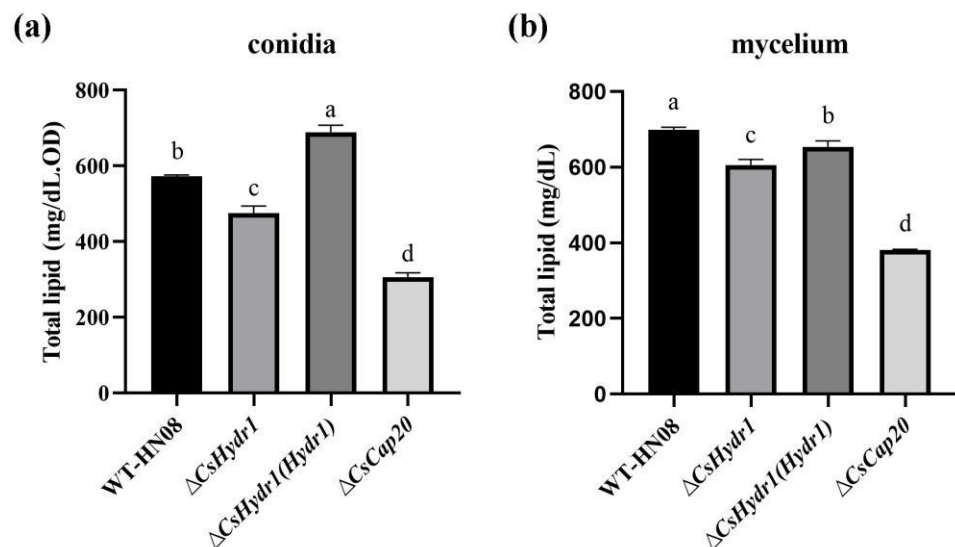


Figure 8. Lipid content relationship of *CsHydr1* and *CsCap20*. Quantification of lipids from conidia (a) and mycelia (b) in HN08, the $\Delta csHydr1$ mutant, the $\Delta csHydr1(Hydr1)$ strain and the $\Delta csCap20$ mutant. Different letters (a, b, c, d) represent significant difference.

4. Discussion

Filamentous fungi generally contain multiple hydrophobin genes, which play important roles in fungal growth, development and environmental communication [26,46–48]. In this study, we cloned the class I hydrophobin family member CsHydr1 in *C. siamense* from *Hevea brasiliensis* and confirmed that CsHydr1 was involved in the morphogenesis of hyphae and conidia, affecting cell wall integrity and pathogenicity in *C. siamense*. Furthermore, we demonstrated that hydrophobin CsHydr1 interacted with the lipid droplet-associated protein CsCap20, which is involved in pathogenicity, localized on the surface of lipid droplets and involved in regulating the content of lipid droplets and affecting pathogenicity.

Hydrophobins are small, secreted proteins and amphiphilic proteins that can self-assemble into monolayers on hydrophobic: hydrophilic interfaces and can form a rodlet layer to be used for surface coatings [49]. Hydrophobins are capable of altering the surface tension and hydrophobicity, which affect the growth of hyphae, including Trhfb3 in *T. reesei* [50], SC3 in *S. commune* [51], Hyd1 and Hyd3 in *C. rosea* [52], and most hydrophobins in *Corioliopsis trogii* [53]. The protein CsHydr1 in *C. siamense* was identified as a secreted protein, and a gene knockout mutant also led to a slight increase in the colony growth rate in this study, suggesting that CsHydr1 may affect surface tension to some extent, which is similar to other known hydrophobins.

However, not all hydrophobins are involved in spore superficial rodlet layers. Here, the subcellular localization of CsHydr1 was significantly different from some other fungal hydrophobins reported. In general, hydrophobins of filamentous fungi are secreted and cover the walls of spores and hyphae with a hydrophobic layer [25]. By their ability to aggregate to amphipathic membranes, they attach to the surface of the hydrophilic fungal cell wall, thereby exposing the hydrophobin layers to the outside, which can often be recognized by the formation of rodlets with scanning electron microscopy [26,45]. For example, six hydrophobins (Rod A, Dew A–E) in *Aspergillus nidulans* all localized on the conidiospore surface involved in hydrophobin rodlet formation and contributed to the hydrophobicity of the spore surface [54]. The absence of RodA caused the loss of the conidial rodlet structure, and other hydrophobins, such as Dew A–E, had minor effects on the Integrity of the rodlet layer [54]. Two hydrophobins, Hyd1 and Hyd2 in *Beauveria bassiana*, were also identified as localizing on the spore surface and were involved in spore coat rodlet layer formation [36]. However, we did not find a rodlet layer on the surface of wild-type spores and did not find a significant difference in the outside layer of the spore between the wild-type strain and Δ CsHydr1. Similar phenotypes were also found in *Botrytis cinerea*; neither the hydrophobin (Bhp1, Bhp2 and Bhp3) triple knockout mutants nor the wild-type conidia were covered with rodlet-shaped structures, and no differences were observed between them [55]. Furthermore, we found that CsHydr1 was significantly localized on the lipid droplet surface and interacted with the lipid-coated protein CsCap20 in *C. siamense*.

Some hydrophobins of plant/entomo-pathogenic fungi are involved in virulence. However, their roles in fungal virulence are different and remain to be understood. Knock-out of *MPG1* in *M. grisea* results in impaired appressorium development and reduced infectivity [32,56]. The deletion of another hydrophobin gene, *MHP1*, in *M. grisea* also led to a loss of viability and a reduced capacity to infect and colonize a susceptible rice cultivar. In *B. bassiana*, the nonspecific hydrophobic interaction between the fungal spore coat hydrophobin and the insect epicuticle is involved in establishing the pathogenicity of the fungus [36]. *FgHyd2*, *FgHyd3* and *FgHyd4* are involved in the adhesion of conidia to wheat spikes during the early stages of the infection process, but *Fghyd1* and *Fghyd5* deletion mutants presented pathogenicity similar to WT [31].

This research confirmed the role of the pathogenicity function of CsHydr1 in *C. siamense*. However, it seems that the mechanism may be different from those of hydrophobins mentioned above. Our findings indicate that CsHydr1 interacts with the lipid droplet-coated protein CsCap20, localizes with intracellular lipid droplets in *C. siamense*, and influences lipid content. However, when CsCap20 was absent, some CsHydr1 was clearly

observed in other parts (Figure 7c), we speculated that CsHydr1 is also localized on other organelles membrane lipid or dissociating lipid, and CsCap20 was helpful for the localization of CsHydr1 on lipid droplets, the interaction between CsHydr1 and CsCap20 is conducive to the formation and stability of lipid droplets in *C. siamense*. Previous studies have shown that the lipid droplet coating protein CsCap20 of *C. siamense* and its homologue Mpl1 in *M. anisopliae* affect the formation of lipid droplets in fungi and affect appressorium turgor and pathogenicity [22,41]. We speculate that CsHydr1 and CsCap20 jointly affect the formation of lipid droplets and the content of lipids, which in turn affect appressorium formation and turgor and further lead to reduced pathogenicity.

Thus, this study confirmed that the hydrophobin CsHydr1 interacts with the lipid droplet coating protein CsCap20 and localizes with lipid droplets and affects the intercellular lipid content of hyphae and spores.

Supplementary Materials: The following supporting information can be downloaded at: <https://www.mdpi.com/article/10.3390/jof8090977/s1>; Figure S1: Schematic representation of the targeted deletion of the *CsHydr1* gene by the homologous recombination method and molecular confirmation; Figure S2: Phylogenetic analysis of protein CsHydr1 and several known hydrophobin proteins in fungi; Table S1: All the primers used in this study.

Author Contributions: Investigation, formal analysis, writing—original draft, N.W. and J.W.; methodology, J.L., Y.L. and Y.X.; validation, M.S. and X.G.; data curation, Z.L.; validation, X.L. and Y.Z.; writing—review and editing; funding acquisition, C.L.; writing—review and editing, W.M. All authors have read and agreed to the published version of the manuscript.

Funding: This research was funded by the Basic and Applied Basic Research Program of Hainan province (No. 2019RC035; 320RC477), the National Natural Science Foundation of China (No. 32160613), and the Earmarked Fund for China Agriculture Research System (No. CARS-33-BC1).

Institutional Review Board Statement: Not applicable.

Informed Consent Statement: Not applicable.

Data Availability Statement: The data that support the findings of this study are available from the corresponding author upon reasonable request.

Acknowledgments: The authors thank the College of Tropical Crops Hainan University for providing a confocal microscope in this work.

Conflicts of Interest: The authors declare no conflict of interest.

References

1. Kim, J.W.; Shim, S.H. The fungus *Colletotrichum* as a source for bioactive secondary metabolites. *Arch. Pharm. Res.* **2019**, *42*, 735–753. [[CrossRef](#)] [[PubMed](#)]
2. Liu, X.; Li, B.; Cai, J.; Zheng, X.; Feng, Y.; Huang, G. *Colletotrichum* species causing anthracnose of rubber trees in China. *Sci. Rep.* **2018**, *8*, 10435. [[CrossRef](#)] [[PubMed](#)]
3. Cao, X.; Xu, X.; Che, H.; West, J.S.; Luo, D. Distribution and fungicide sensitivity of *Colletotrichum* species complexes from rubber tree in Hainan, China. *Plant Dis.* **2017**, *101*, 1774–1780. [[CrossRef](#)] [[PubMed](#)]
4. Du, Y.; Wang, M.; Zou, L.; Long, M.; Yang, Y.; Zhang, Y.; Liang, X. Quantitative Detection and Monitoring of *Colletotrichum siamense* in Rubber Trees Using Real-Time PCR. *Plant Dis.* **2021**, *105*, 2861–2866. [[CrossRef](#)]
5. Qin, L.; Huang, S.; Lin, S.; Lin, C. First report of anthracnose of *Mangifera indica* caused by *Colletotrichum siamense* in Sanya city in China. *Plant Dis.* **2017**, *101*, 1038. [[CrossRef](#)]
6. Ling, J.; Song, X.; Xi, P.; Cheng, B.; Cui, Y.; Chen, X.; Peng, A.; Jiang, Z.; Zhang, L. Identification of *Colletotrichum siamense* causing litchi pepper spot disease in mainland China. *Plant Pathol.* **2019**, *68*, 1533–1542. [[CrossRef](#)]
7. Zhao, J.; Liu, T.; Zhang, D.; Wu, H.; Pan, L.; Liao, N.; Liu, W. First report of anthracnose caused by *Colletotrichum siamense* and *C. fructicola* of *Camellia chrysantha* in China. *Plant Dis.* **2021**, *105*, 2020. [[CrossRef](#)]
8. Shu, J.; Guo, T.; Li, Q.; Tang, L.; Huang, S.; Mo, J.; Yu, Z.; Vivian, P. First report of leaf spot caused by *Colletotrichum fructicola* and *C. siamense* on *Ziziphus mauritiana* in Guangxi, China. *Plant Dis.* **2021**, *105*, 2021. [[CrossRef](#)]
9. Huang, R.; Sun, W.; Li, W.; Zhou, C.; Huang, S.; Tang, L.; Li, Q.; Guo, T.; Mo, J.; Ning, P. First report of *Colletotrichum siamense* causing leaf spot on *Alocasia macrorrhiza* in China. *Plant Dis.* **2021**, *105*, 1857. [[CrossRef](#)]
10. Weir, B.S.; Johnston, P.R.; Damm, U. The *Colletotrichum gloeosporioides* species complex. *Stud. Mycol.* **2012**, *73*, 115–180. [[CrossRef](#)]

11. Mendgen, K.; Hahn, M.; Deising, H. Morphogenesis and mechanisms of penetration by plant pathogenic fungi. *Annu. Rev. Phytopathol.* **1996**, *34*, 367–386. [\[CrossRef\]](#)
12. de Jong, J.C.; McCormack, B.J.; Smirnov, N.; Talbot, N.J. Glycerol generates turgor in rice blast. *Nature* **1997**, *389*, 244. [\[CrossRef\]](#)
13. Sangappillai, V.; Nadarajah, K. Fatty acid synthase beta dehydratase in the lipid biosynthesis pathway is required for conidiogenesis, pigmentation and appressorium formation in *Magnaporthe oryzae* S6. *Int. J. Mol. Sci.* **2020**, *21*, 7224. [\[CrossRef\]](#)
14. Auyong, A.S.; Ford, R.; Taylor, P.W. The role of cutinase and its impact on pathogenicity of *Colletotrichum truncatum*. *J. Plant Pathol. Microb.* **2015**, *6*. [\[CrossRef\]](#)
15. Wang, Z.; Soanes, D.M.; Kershaw, M.J.; Talbot, N.J. Functional analysis of lipid metabolism in *Magnaporthe grisea* reveals a requirement for peroxisomal fatty acid β -oxidation during appressorium-mediated plant infection. *Mol. Plant Microbe Interact.* **2007**, *20*, 475–491. [\[CrossRef\]](#)
16. Bickel, P.E.; Tansey, J.T.; Welte, M.A. PAT proteins, an ancient family of lipid droplet proteins that regulate cellular lipid stores. *Biochim. Biophys. Acta* **2009**, *1791*, 419–440. [\[CrossRef\]](#)
17. Martinez-Botas, J.; Anderson, J.B.; Tessier, D.; Lapillonne, A.; Chang, B.H.; Quast, M.J.; Gorenstein, D.; Chen, K.H.; Chan, L. Absence of perilipin results in leanness and reverses obesity in *Leprdb/db* mice. *Nat. Genet.* **2000**, *26*, 474–479. [\[CrossRef\]](#)
18. Tansey, J.T.; Sztalryd, C.; Gruia-Gray, J.; Roush, D.L.; Zee, J.V.; Gavrilova, O.; Reitman, M.L.; Deng, X.C.; Li, C.; Kimmel, R.A.; et al. Perilipin ablation results in a lean mouse with aberrant adipocyte lipolysis, enhanced leptin production, and resistance to diet-induced obesity. *Proc. Natl. Acad. Sci. USA* **2001**, *98*, 6494–6499. [\[CrossRef\]](#)
19. Tansey, J.; Sztalryd, C.; Hlavin, E.; Kimmel, A.; Londos, C. The central role of perilipin a in lipid metabolism and adipocyte lipolysis. *IUBMB Life* **2004**, *56*, 379–385. [\[CrossRef\]](#)
20. Wang, C.; ST Legar, R.J. The *Metarhizium anisopliae* perilipin homolog MPL1 regulates lipid metabolism, appressorial turgor pressure, and virulence. *J. Biol. Chem.* **2007**, *282*, 21110–21115. [\[CrossRef\]](#)
21. Hwang, C.S.; Flaishman, M.A.; Kolattukudy, P.E. Cloning of a gene expressed during appressorium formation by *Colletotrichum gloeosporioides* and a marked decrease in virulence by disruption of this gene. *Plant Cell* **1995**, *7*, 183–193. [\[CrossRef\]](#)
22. Lin, C.; Liu, X.; Shi, T.; Li, C.; Huang, G. The *Colletotrichum gloeosporioides* perilipin homologue CAP 20 regulates functional appressorial formation and fungal virulence. *J. Phytopathol.* **2018**, *166*, 216–225. [\[CrossRef\]](#)
23. Wang, J.; Zhao, X.; Liao, X.; He, Q.; Li, X.; Liu, W.; Yang, Z.; Zhang, Y.; Lin, C.; Miao, W. Screening for proteins interacting with the perilipin-like protein CAP20 by a yeast two-hybrid system and identification of a protein kinase a catalytic subunit as an interacting protein in *Colletotrichum siamense*. *Eur. J. Plant Pathol.* **2020**, *156*, 971–977. [\[CrossRef\]](#)
24. Shin, Y.K.; Kim, D.W.; Lee, S.W.; Lee, M.J.; Baek, S.G.; Lee, T.; Yun, S.H. Functional roles of all five putative hydrophobin genes in growth, development, and secondary metabolism in *Fusarium graminearum*. *Fungal Genet. Biol.* **2022**, *160*, 103683. [\[CrossRef\]](#)
25. Wessels JG, H. Fungal hydrophobins: Proteins that function at an interface. *Trends Plant Sci.* **1996**, *1*, 9–15. [\[CrossRef\]](#)
26. Wösten, H.A. Hydrophobins: Multipurpose proteins. *Annu. Rev. Microbiol.* **2001**, *55*, 625–646. [\[CrossRef\]](#)
27. Li, X.; Wang, F.; Xu, Y.; Liu, G.; Dong, C. Cysteine-rich hydrophobin gene family: Genome wide analysis, phylogeny and transcript profiling in *Cordyceps militaris*. *J. Mol. Sci.* **2021**, *22*, 643. [\[CrossRef\]](#)
28. Wösten, H.A.; Wessels, J.G. Hydrophobins, from molecular structure to multiple functions in fungal development. *Mycoscience* **1997**, *38*, 363–374. [\[CrossRef\]](#)
29. Askolin, S.; Penttilä, M.; Wösten, H.A.; Nakari-Setälä, T. The *Trichoderma reesei* hydrophobin genes *hfb1* and *hfb2* have diverse functions in fungal development. *FEMS Microbiol. Lett.* **2005**, *253*, 281–288. [\[CrossRef\]](#) [\[PubMed\]](#)
30. Fuchs, U.; Czymbek, K.J.; Sweigard, J.A. Five hydrophobin genes in *Fusarium verticillioides* include two required for microconidial chain formation. *Fungal Genet. Biol.* **2004**, *41*, 852–864. [\[CrossRef\]](#) [\[PubMed\]](#)
31. Quarantin, A.; Hadelger, B.; Kröger, C.; Schäfer, W.; Favaron, F.; Sella, L.; Martínez-Rocha, A.L. Different hydrophobins of *Fusarium graminearum* are involved in hyphal growth, attachment, water-air interface penetration and plant infection. *Front. Microbiol.* **2019**, *10*, 751. [\[CrossRef\]](#)
32. Talbot, N.J.; Kershaw, M.J.; Wakley, G.E.; De Vries, O.M.; Wessels, J.G.; Hamer, J.E. MPG1 encodes a fungal hydrophobin involved in surface interactions during infection-related development of *Magnaporthe grisea*. *Plant Cell* **1996**, *8*, 985–999. [\[CrossRef\]](#)
33. Inoue, K.; Kitaoka, H.; Park, P.; Ikeda, K. Novel aspects of hydrophobins in wheat isolate of *Magnaporthe oryzae*: Mpg1, but not Mhp1, is essential for adhesion and pathogenicity. *J. Gen. Plant Pathol.* **2016**, *82*, 18–28. [\[CrossRef\]](#)
34. Kim, S.; Ahn, I.P.; Rho, H.S.; Lee, Y.H. MHP1, a *Magnaporthe grisea* hydrophobin gene, is required for fungal development and plant colonization. *Mol. Microbiol.* **2005**, *57*, 1224–1237. [\[CrossRef\]](#)
35. Soanes, D.M.; Kershaw, M.J.; Cooley, R.N.; Talbot, N.J. Regulation of the MPG1 hydrophobin gene in the rice blast fungus *Magnaporthe grisea*. *Mol. Plant Microbe Interact.* **2002**, *15*, 1253–1267. [\[CrossRef\]](#)
36. Zhang, S.; Xia, Y.X.; Kim, B.; Keyhani, N.O. Two hydrophobins are involved in fungal spore coat rodlet layer assembly and each play distinct roles in surface interactions, development and pathogenesis in the entomopathogenic fungus, *Beauveria bassiana*. *Mol. Microbiol.* **2011**, *80*, 811–826. [\[CrossRef\]](#)
37. Lin, C.; Huang, G.; Zheng, F.; Miao, W. Functional characterization of CgPBS2, a MAP kinase kinase in *Colletotrichum gloeosporioides*, using osmotic stress sensitivity as a selection marker. *Eur. J. Plant Pathol.* **2018**, *152*, 801–813. [\[CrossRef\]](#)
38. Song, M.; Fang, S.; Li, Z.; Wang, N.; Li, X.; Liu, W.; Miao, W. CsAtf1, a bZIP transcription factor, is involved in fludioxonil sensitivity and virulence in the rubber tree anthracnose fungus *Colletotrichum siamense*. *Fungal Genet. Biol.* **2022**, *158*, 103649. [\[CrossRef\]](#)

39. Tamura, K.; Stecher, G.; Peterson, D.; Filipinski, A.; Kumar, S. MEGA6: Molecular Evolutionary Genetics Analysis Version 6.0. *Mol. Biol. Evol.* **2013**, *30*, 2725–2729. [[CrossRef](#)]
40. Li, X.; Liu, Y.; He, Q.; Li, S.; Liu, W.; Lin, C.; Miao, W. A candidate secreted effector protein of rubber tree powdery mildew fungus contributes to infection by regulating plant ABA biosynthesis. *Front. Microbiol.* **2020**, *11*, 591387. [[CrossRef](#)]
41. Wösten, H.A.; de Vocht, M.L. Hydrophobins, the fungal coat unravelled. *Bioch. Biophys. Acta* **2000**, *1469*, 79–86. [[CrossRef](#)]
42. Jensen, B.G.; Andersen, M.R.; Pedersen, M.H.; Frisvad, J.C.; Søndergaard, I. Hydrophobins from *Aspergillus* species cannot be clearly divided into two classes. *BMC Res. Notes* **2010**, *3*, 344. [[CrossRef](#)] [[PubMed](#)]
43. Jacobs, K.A.; Collins-Racie, L.A.; Colbert, M.; Duckett, M.; Golden-Fleet, M.; Kelleher, K.; McCoy, J.M. A genetic selection for isolating cDNAs encoding secreted proteins. *Gene* **1997**, *198*, 289–296. [[CrossRef](#)]
44. Oh, S.K.; Young, C.; Lee, M.; Oliva, R.; Bozkurt, T.O.; Cano, L.M.; Kamoun, S. In planta expression screens of *Phytophthora infestans* RXLR effectors reveal diverse phenotypes, including activation of the *Solanum bulbocastanum* disease resistance protein Rpi-blb2. *Plant Cell* **2009**, *21*, 2928–2947. [[CrossRef](#)] [[PubMed](#)]
45. Kwan, A.H.Y.; Winefield, R.D.; Sunde, M.; Matthews, J.M.; Haverkamp, R.G.; Templeton, M.D.; Mackay, J.P. Structural basis for rodlet assembly in fungal hydrophobins. *Proc. Natl. Acad. Sci. USA* **2006**, *103*, 3621–3626. [[CrossRef](#)] [[PubMed](#)]
46. Wessels, J.G. Hydrophobins: Proteins that change the nature of the fungal surface. *Adv. Microb. Physiol.* **1996**, *38*, 1–45. [[CrossRef](#)]
47. Whiteford, J.R.; Spanu, P.D. Hydrophobins and the interactions between fungi and plants. *Mol. Plant Pathol.* **2002**, *3*, 391–400. [[CrossRef](#)] [[PubMed](#)]
48. Bayry, J.; Aimanianda, V.; Guijarro, J.I.; Sunde, M.; Latge, J.P. Hydrophobins—Unique fungal proteins. *PLoS Pathog.* **2012**, *8*, e1002700. [[CrossRef](#)]
49. Wenandy, L.; Hilpert, F.; Schlebusch, O.; Fischer, R. Comparative analysis of surface coating properties of five hydrophobins from *Aspergillus nidulans* and *Trichoderma reesei*. *Sci. Rep.* **2018**, *8*, 12033. [[CrossRef](#)]
50. He, R.; Li, C.; Feng, J.; Zhang, D. A class II hydrophobin gene, *Trhfb3*, participates in fungal asexual development of *Trichoderma reesei*. *FEMS Microbiol. Lett.* **2017**, *364*. [[CrossRef](#)]
51. Wessels, J.G.; De Vries, O.M.; Asgeirsdottir, S.A.; Schuren, F. Hydrophobin genes involved in formation of aerial hyphae and fruit bodies in *Schizophyllum*. *Plant Cell* **1991**, *3*, 793–799. [[CrossRef](#)]
52. Dubey, M.K.; Jensen, D.F.; Karlsson, M. Hydrophobins are required for conidial hydrophobicity and plant root colonization in the fungal biocontrol agent *Clonostachys rosea*. *BMC Microbiol.* **2014**, *14*, 18. [[CrossRef](#)]
53. Wang, L.; Lu, C.; Fan, M.; Liao, B. *Corioloropsis trogii* hydrophobin genes favor a clustering distribution and are widely involved in mycelial growth and primordia formation. *Gene* **2021**, *802*, 145863. [[CrossRef](#)]
54. Grünbacher, A.; Throm, T.; Seidel, C.; Cutt, B.; Röhrig, J.; Strunk, T.; Fischer, R. Six hydrophobins are involved in hydrophobin rodlet formation in *Aspergillus nidulans* and contribute to hydrophobicity of the spore surface. *PLoS ONE* **2014**, *9*, e94546. [[CrossRef](#)]
55. Mosbach, A.; Leroch, M.; Mendgen, K.W.; Hahn, M. Lack of evidence for a role of hydrophobins in conferring surface hydrophobicity to conidia and hyphae of *Botrytis cinerea*. *BMC Microbiol.* **2011**, *11*, 10. [[CrossRef](#)]
56. Talbot, N.J.; Ebole, D.J.; Hamer, J.E. Identification and characterization of MPG1, a gene involved in pathogenicity from the rice blast fungus *Magnaporthe grisea*. *Plant Cell* **1993**, *5*, 1575–1590. [[CrossRef](#)]